Front. Optoelectron. 2020, 13(1): 18–34
https://doi.org/10.1007/s12200-019-0942-1

REVIEW ARTICLE

Distributed feedback organic lasing in photonic crystals

Yulan FU, Tianrui ZHAI (✉)

Institute of Information Photonics Technology, College of Applied Sciences, Beijing University of Technology, Beijing 100124, China

Abstract Considerable research efforts have been devoted to the investigation of distributed feedback (DFB) organic lasing in photonic crystals in recent decades. It is still a big challenge to realize DFB lasing in complex photonic crystals. This review discusses the recent progress on the DFB organic laser based on one-, two-, and three-dimensional photonic crystals. The photophysics of gain materials and the fabrication of laser cavities are also introduced. At last, future development trends of the lasers are prospected.

Keywords photonic crystals, microcavity lasers, distributed feedback (DFB)

1 Introduction

Photonic crystals, proposed by Yablonovitch [1] and John [2], have shown great potential for developing different photonic devices [3–5]. Great interest is focused on realizing the photonic band gap and the photonic localization of photonic crystals [6–8]. In the photonic band gap, the propagation of electromagnetic waves inside the photonic crystals is forbidden in all directions. It provides new possibilities for us to control the behavior of electromagnetic waves. Especially, the controllability of the optical density of modes helps us realize the enhancement of emission at the photonic band edge [9–11]. Based on this characteristic, much work has so far focused on potential applications in the fields of nanoscale lasers [12–14], optical switching [15–17], optical logic gates [18–20], gap solitons [21–23], sensors [24–26], and so on.

Since the pioneering work of Painter et al. [27], a significant effort has been devoted to the development of nanoscale lasers based on photonic crystals. The nanoscale lasers can be divided into two types: photonic band-gap defect mode lasers [27–29] and photonic band edge lasers [30–32]. The former has a resonant cavity with a defect and laser oscillations origin from the resonant modes of the cavity. The latter has a resonant cavity without defects and lasing actions are enhanced by the optical density of modes at the band edge of photonic crystals.

A low threshold is an intrinsical feature of photonic band edge lasers [33]. It can be attributed to the low loss and high gain of the laser system. For photonic band edge lasers, the loss includes from the propagation loss and the radiation loss [30]. Generally, the propagation loss is very small for the photonic band edge lasers due to the extremely slow group velocity near the photonic band edges. The radiation loss mainly exists in one- (1D) and two- (2D) dimensional photonic crystals due to the poor confinement of light in a certain dimension. In theory, the radiation loss is quite small in the three-dimensional (3D) case because the 3D photonic bandgap enables a 3D confinement of light. The gain in the photonic band edge lasers will be discussed in detail later.

Photonic band edge lasers can be divided into two categories: lasers based on the guided modes and lasers based on the waveguide modes. For lasers based on the guided modes, the guided mode is related to the photonic band gap of photonic crystals. A photonic crystal acts as the laser cavity [34,35]. For lasers based on the waveguide modes, the waveguide mode is determined by a combination of a waveguide and a "photonic crystal" with weak modulation [36–38]. The latter is often referred to as the distributed feedback (DFB) lasers [39–41]. For 1D and 2D cases, the "photonic crystal" with weak modulation is known as "gratings". The laser cavity consists of a grating and a waveguide [42–44]. The nature of the photonic band edge lasers can be explained by the dispersion relations in the laser cavity [36,45].

Furthermore, the development of gain materials has a great influence on the development of lasers. On the one hand, it can improve the performance of lasers; on the other hand, it can hasten new lasers. The gain materials involved in DFB lasers include organic semiconductors, inorganic semiconductors, dyes, quantum dots, perovskite, carbon dots, and so on. Due to the rapid development of the gain

Received June 10, 2019; accepted August 11, 2019

E-mail: trzhai@bjut.edu.cn

materials, it is impossible to review completely the most relevant advances. This review focuses on characteristics of organic semiconductors, organic dyes, and semiconductor quantum dots.

In this paper, we briefly review some advances in DFB lasers in 1D, 2D, and 3D photonic crystals. We discuss photophysics of gain materials, design and fabrication of laser cavity, principles of modeling feedback mechanisms, and progress toward applications. The trends and challenges for DFB polymer lasers have also been discussed.

2 Gain materials

As one of the most important components of the laser system, gain materials play a crucial role in the laser performance. Some gain materials open up the prospect of high-performance lasers suitable for real applications. Inorganic semiconductor lasers dominate the laser applications for several decades [46–48]. However, the common inorganic semiconductor lasers cannot cover the whole visible spectral region. Dye lasers are investigated almost simultaneously with the discovery of the laser, which operates using dye molecules [49]. In addition, as a gain material with a zero-dimensional density of states, quantum dots were applied to lasers successfully in the 1990s [50–52]. There are some differences between organic semiconductors, organic dyes, and semiconductor quantum dots, including the film-forming property, electrical conductivity, and the difficulty of manufacturing. Recently, some new materials have been developed and introduced to lasers, such as perovskites [53–55], carbon nanodots [56,57]. We will not address these breathtaking advances in this paper.

2.1 Organic semiconductors

Organic semiconductors are usually chain-like molecules, which can be regarded as arrays of randomly oriented chromophores consisted of conjugated segments. The segment comprises a huge number of fundamental repeat units. The photophysical property of the material origins from the overlap of the molecular orbitals, which can be revealed by the time-resolved measurements. According to the molecular structure, organic semiconductors can be classified into small molecules (molecular weight $< 10^3$) [58–60], macromolecules [61–63], and polymers (molecular weight $< 10^4$) [64–66]. Small molecules include conjugated and non-conjugated molecules, organic metal complexes, and so on. Macromolecules include oligomers, starburst molecules, and dendrimers. Polymers include the poly(phenylenevinylene)s [67–69], the ladder-type poly (para-phenylene) [70–72], the polyfluorenes [73–75], and so on.

As an attractive gain material, organic semiconductors show rich and broad emission spectra from the near ultraviolet to infrared, large Stokes shift, strong absorption coefficients (~10^5 cm^{-1}), low quenching rate at high concentrations, high fluorescence quantum efficiencies, and perfect charge transport properties. Rich and broad emission spectra enable the possibility of multi-wavelength emissions and tunable lasers. Large Stokes shift avoids the absorption of emission lights. Strong absorption coefficients imply a strong amplification of emission lights. Low quenching rate at high concentrations facilitates the easy fabrication of neat solid films. High fluorescence quantum efficiencies bring about excellent performances including low thresholds and high slope efficiencies. Perfect charge transport properties provide the potential to realize electrically pumped laser devices. Most of the features are derived from the enormous range of customizable structures. Moreover, the simple fabrication and flexibility of organic semiconductors provide more opportunities for electronics and optoelectronics.

The stimulated emission is firstly observed in a conjugated polymer film of poly(p-phenylene vinylene,

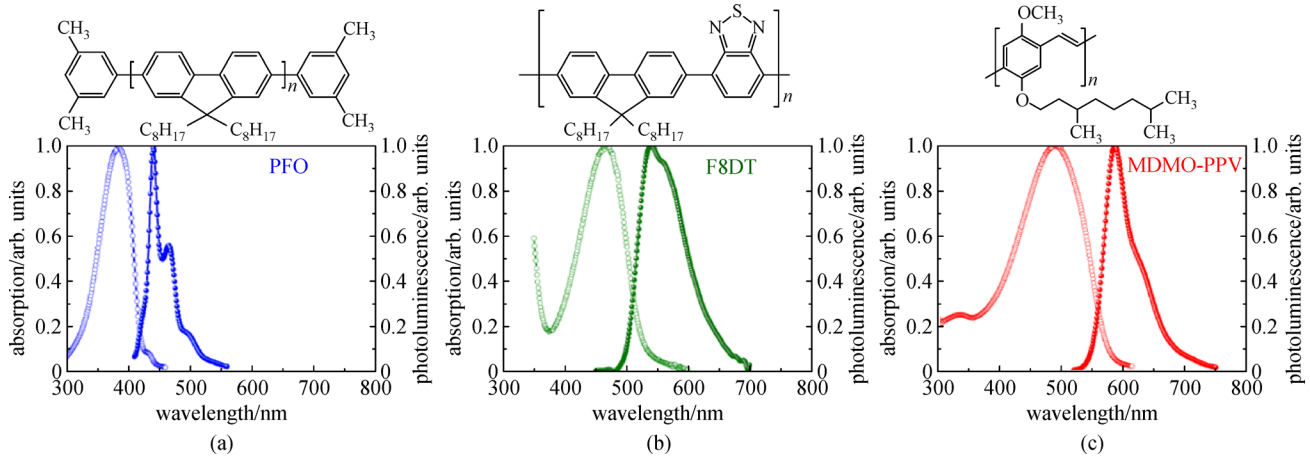

Fig. 1 Absorption and PL spectra of (a) PFO, (b) F8BT, and (c) MDMO-PPV. The upper panel presents the corresponding molecular structure. Reproduced with permission [80]. Copyright 2015, RSC Publishing

PPV) [76]. Nowadays, there are plenty of polymers that are widely used in lasing applications. In this paper, we mainly focus on three types of polymers, poly[9,9-dioctylfl uorenyl-2,7-diyl]–end capped with DMP (PFO, American Dye Source), poly[(9,9-dioctylfluorenyl-2,7-diyl)-alt-co-(1,4-benzo-(2,1′,3) -thiadiazole)] (F8BT, American Dye Source), and poly[2-methoxy-5-(3′,7′-dimethyloctyloxy)-1,4-phenylenevinylene] (MDMO-PPV, Sigma-Aldrich). The absorption (open circles) and photoluminescence (PL, close circles) spectra of PFO, F8BT, and MDMO-PPV are plotted in Fig. 1, respectively. Note that the Stokes shift (the deviation between the absorption and PL spectra) is large enough to avoid the absorption of emission lights. The upper panels of Fig. 1 show the molecular structures. The net gain coefficient of PFO, F8BT, MDMO-PPV are about 74, 26, 50 cm^{-1}, respectively [77–79].

2.2 Organic dyes

Almost with the invention of the laser, the organic dyes came to people's attention. The dye laser action was firstly reported in 1966 [81]. After years of rapid development, the organic dye laser becomes a powerful tool for the development in the areas of physics, chemistry, and materials. Dyes are a class of colored materials which can impart color to other materials. Later organic compounds are included in the dyes, such as rhodamine 6G. Generally, the molecular weight of dyes is about several hundreds. Spectral narrowing effect can be observed in hundreds of organic dyes under pumping conditions. The emission wavelength varies from 190 to 1850 nm. Dyes include cyanine dyes [82–84], oxazine dyes [85–87], coumarin dyes [88–90], rhodamine dyes [91–93], and so on.

The advantages of dyes are strong absorptions, near unity quantum efficiency, broad spectra, excellent tunability, and easy fabrications. However, the dye is non-conductive, which is regarded as the main obstacle for realizing electrically pumping laser devices. Most optical behaviors of dyes can be understood by a quasi-four-level model [49]. For laser applications, the state of dyes can be solid, liquid, and gas. Figure 2 presents the absorption (dotted curves) and PL (solid curves) spectra of three common laser dyes, coumarin 440 (C440), coumarin 153 (C153), and rhodamine 6G (R6G).

2.3 Semiconductor quantum dots

Quantum dots (QDs) are tiny clusters of semiconductors with dimensions of only several nanometers. The great potential of semiconductor QDs as gain materials for laser applications has been recognized since the appearance of QDs laser [94–96]. Nowadays, semiconductor QDs lasers are regarded as highly efficient and compact light sources. The direct electrical control of QDs lasers has also been realized. Two classes of QDs are very promising for laser devices [52]. One is III-V QDs, such as InGaAs/InAs QDs. The other is semiconductor nanoparticles, such as PbS and CdTe. Usually, the former is fabricated on a semiconductor substrate. The latter is incorporated with transparent dielectric matrices.

The advantages of semiconductor QDs are ultrafast carrier dynamics, low threshold current density, broadband gain and absorption, and high PL quantum yield. Such device designs have opened up new possibilities in ultrafast science and technology. The semiconductor QDs is sensitive to the temperature due to the high mobility, and the fabrication method of QDs devices is complicated compared with that of its counterparts mentioned above. Figure 3 demonstrates the absorption (open circles) and PL (solid circles) spectra of three common QDs, ZnCdS/ZnS CQDs, CdSe/ZnS CQDs, and CdSe/CdS/ZnS CQDs.

3 Laser cavities

The principal parts of a laser are the pump, the gain material, and the cavity. The pump supplies energy for the laser to operate, which includes optical pumping and electrical pumping. Prospects for the pump will be discussed later. The gain materials mentioned above amplify the light by simulated emission, which affects the temporal characteristics and the power characteristics of the laser. The cavity provides feedback of the light,

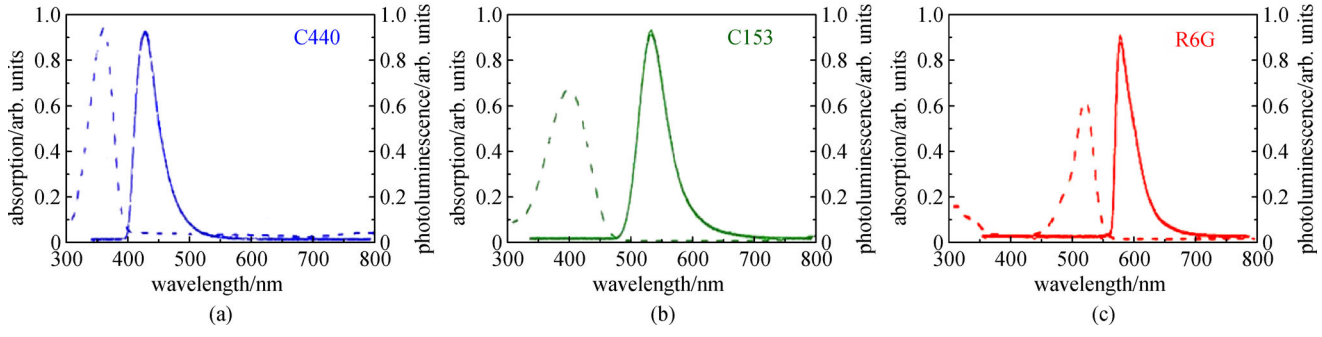

Fig. 2 Absorption and PL spectra of (a) coumarin 440, (b) coumarin 153, and (c) rhodamine 6G. Reproduced with permission [90]. Copyright 2014, OSA Publishing

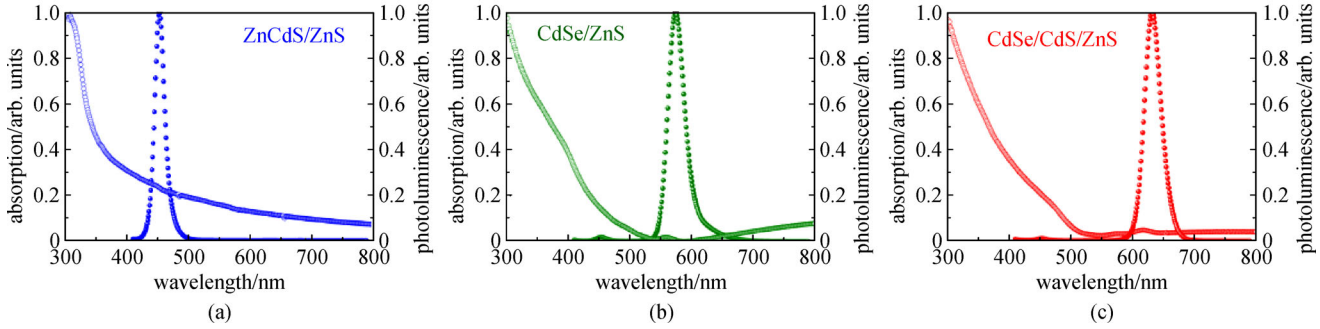

Fig. 3 Absorption and PL spectra of (a) blue QDs, (b) green QDs, and (c) red QDs

which effectively increases the optical path of the light through the gain materials to build up the laser oscillation. The cavity defines the frequency characteristics, the spatial characteristics, and the power characteristics of the laser. The frequency characteristics include the longitudinal, or axial, modes of the cavity, and the linewidth. The spatial characteristics include the pattern, polarization, and beam divergence of the laser. The power characteristics include the laser threshold and output efficiency. Generally speaking, the main parameters of the cavity contain the type, the material, the quality, and the size.

The most common cavity types can be divided into four categories: Fabry-Perot (FP) cavity [97–99], whispering-gallery-mode (WGM) cavity [100–102], distributed-Bragg-reflector (DBR) cavity [103–105], and DFB cavity [106,107], as shown in Fig. 4. There are periodic structures in the DBR cavity and DFB cavity. So, the lasing action in the DBR cavity and DFB cavity can be explained by the theory of photonic crystals. This review will focus on the DFB cavity. Recently, the compound cavity has begun to receive research attention, which can be regarded as a combination of several common cavity types [108–110].

The cavity supports a discrete set of wavelengths, which are also called the resonant wavelengths (frequencies). The relationship between the optical path of the cavity (P) and the resonant wavelength (λ) is described as $P = k\lambda/2$, where k is an integer. The discreteness of resonant wavelength origins from the boundary condition of the light in the cavity. The phase of light must be exactly the same after a round-trip propagation in the cavity. This is the major reason that most of the characteristics depend on the cavity. Moreover, the allowed resonant frequencies of the laser must be within the PL spectrum of the gain material. More strictly, to build up a stable oscillation of the laser mode, the gain should not be smaller than the loss in one round-trip of the cavity. Thus, in order to achieve lasing, the cavity must be designed carefully. The mode of the cavity should match the gain spectra of the material.

3.1 Types of laser cavities

As mentioned above, various cavity configurations are proposed to design the laser devices. Among them, the DFB cavity is regarded as the most promising solution for

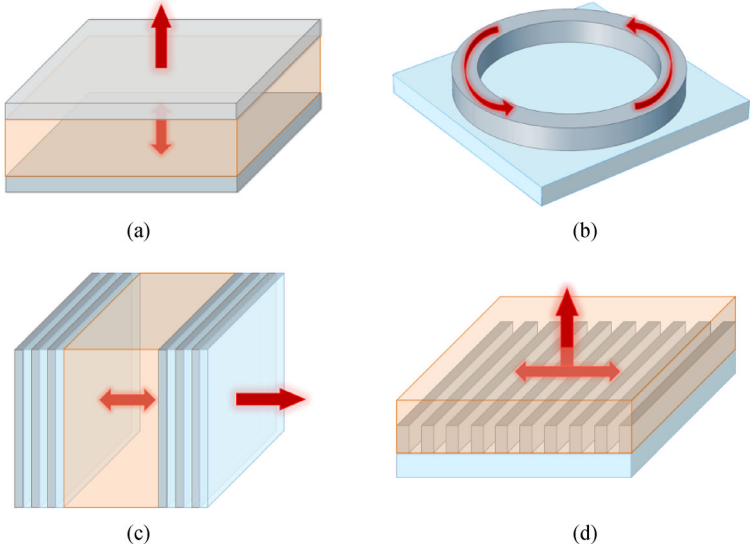

Fig. 4 Schematics of various cavity types. (a) FP cavity; (b) WGM cavity; (c) DBR cavity; (d) DFB cavity

realizing electrically pumped polymer lasers. Therefore, in the rest of this section, we will focus on the DFB cavity and summarize progress in design, fabrication, and feedback mechanism of the DFB cavity type.

According to the spatial structure, DFB cavities can be divided into 1D [111], 2D, and 3D structures. According to the transnational symmetry, DFB cavities can be divided into periodic, quasi-periodic, and aperiodic structures. Moreover, the DFB cavities can be divided into dielectric and metallic structures. Overall, the basic motivation for developing different laser cavities is to achieve a rich variety of temporal, spatial, spectral, and power properties. Figure 5 demonstrates the photonic crystals which can be employed as the DFB cavity. Theoretically, the random structure in Fig. 5(i) is not a DFB structure, which is usually used as a feedback cavity of random lasers [93]. Many irregular closed-loop paths can be excited in the cavity, which may support certain oscillation modes. Since the feedback mechanism of random lasers is quite different from that of DFB lasers [112,113], we will not address the random structure in detail.

1D – 3D structures include gratings/complex lattices [114,115], quasi-crystals [116–118], chirped grating/gradual periodic structures [119], circular structure [120,121], spiral structure [122]. Note that 3D structures can be composed of several 1D/2D structures. All these structures can be employed as DFB cavities.

3.2 Design of laser cavities

The main objectives of the design of laser cavities are to match the gain materials and to control the output characteristics. Several theories are developed to explore the property of DFB lasers, such as the diffraction theory, the couple wave theory, and the photonic bandgap theory. These theories provide a top-down approach to design the laser cavities.

According to the diffraction theory, there are three main roles of cavities, the feedback, the output coupling, and the waveguide. Some characteristics of DFB lasers can be obtained by employing the diffraction theory, such as output directions, output wavelengths, and mode numbers.

As shown in Fig. 6, a typical 1D DFB cavity consists of a grating and a waveguide. The waveguide plays two roles, guiding wave and providing gain. In Fig. 6(a), the red curve denotes the profile of the waveguide mode. Note that there exists a propagating mode and its counter propagating waveguide mode due to the diffraction of the grating [124]. The solid and dashed arrows indicate the feedback and the output direction, respectively. In Fig. 6(b), the red

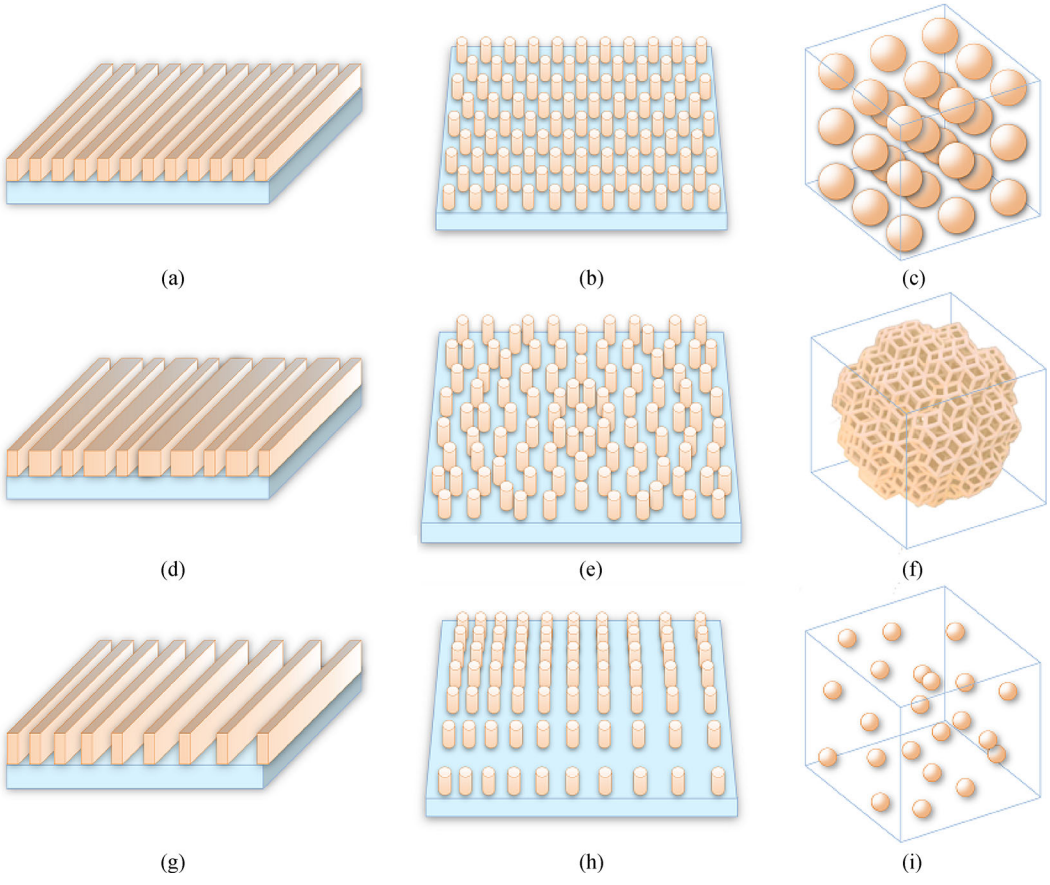

Fig. 5 Photonic crystals for DFB cavities. (a) 1D gratings; (b) 2D periodic structure; (c) 3D periodic structure; (d) Fibonacci quasi-crystals; (e) 2D quasi-crystals; (f) 3D quasi-crystals; (g) Chirped gratings; (h) 2D gradual periodic structure; (i) 3D random structure

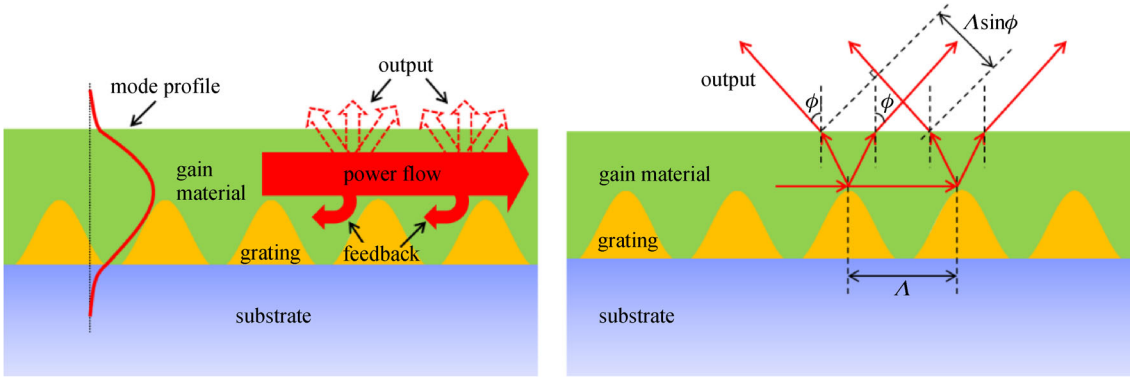

Fig. 6 (a) Schematic of the feedback and the outcoupling of the waveguide mode; (b) diffraction theory of DFB lasers. Reproduced with permission [123]. Copyright 2019, MDPI

arrows present the ray tracing of the propagating and emitting light. It is a simple diffraction picture.

The wavelengths of the waveguide mode must satisfy the Bragg condition in the cavity.

$$2n_{\text{eff}}\Lambda = m\lambda. \tag{1}$$

Here, n_{eff} is the effective refractive index of the waveguide mode, Λ is the grating period, m is a positive integer representing the number of standing wave nodes formed by the propagating and counterpropagating waveguide modes, and λ is the wavelength of the waveguide mode. The guided wave is diffracted by the grating at an angle ϕ, forming the laser output as shown in Fig. 6. The emitted light should satisfy the condition of constructive interference:

$$\frac{2\pi n_{\text{eff}}}{\lambda}\Lambda + \frac{2\pi}{\lambda}\Lambda\sin\phi = 2\pi l, \tag{2}$$

where l is an integer that represents the diffraction order. By substituting Eq. (1) into Eq. (2), the relationship between the output direction of light and the diffraction order is obtained as

$$\frac{\sin\phi}{n_{\text{eff}}} = \frac{2l}{m} - 1,\ l \in [0,m]. \tag{3}$$

Take the case of 1D gratings, the feedback is established by mth order diffraction, whereas the output coupling is supported by different diffraction with order numbers below or equal to m.

The mode number is decided by the parameter of the waveguide. For a given waveguide, there exist the critical thicknesses for the transverse electric mode (TE) and the transverse magnetic mode (TM), respectively. For the mth order TE mode (TE_m), the critical thickness of the waveguide d_{TE} is given by

$$d_{\text{TE}} = \frac{(2m-1)\lambda}{4\sqrt{\varepsilon - 1}}, \tag{4}$$

for the mth order TM mode (TM_m), the critical thickness of the waveguide d_{TM} is given by

$$d_{\text{TM}} = \frac{m\lambda}{2\sqrt{\varepsilon - 1}}, \tag{5}$$

where ε is the effective refractive dielectric constant. According to the relationship of the waveguide mode with the waveguide thickness in Eqs. (4) and (5), if the waveguide thickness is larger than or equal to the critical thicknesses (d_{TE} or d_{TM}), additional modes can be excited.

Under uncoupling conditions, 2D and 3D DFB cavities can be considered as a linear combination of 1D DFB cavities. Therefore, the diffraction theory is applicable to high dimensional cases.

The coupled wave theory reveals most of the physical mechanisms of DFB lasers, such as resonant mode patterns, mode selectivity, differential quantum efficiency, threshold conditions, and effects of end reflections [125–127]. Even under approximate conditions, the couple wave theory can be used to investigate the mode intensity distribution, the lasing wavelength, and the effective refractive index [128–130]. Here, takes an analytical approach for example, it is a combination of the coupled wave theory with the waveguide theory. The physical picture of this method is the resonant mode should meet both the Bragg condition and the waveguide condition.

Figure 7(a) presents a typical cavity, which consists of a grating and a gain waveguide. The cavity is reduced to a four-layered waveguide structure in Fig. 7(b). The electric field distribution in four waveguides in Fig. 7(b) can be defined as [129]

$$E_y(x,z) = \mathrm{e}^{-\mathrm{i}k_z x}\begin{cases} E_1\mathrm{e}^{a_1 x},\ x\in(-\infty,d], \\ E_2\mathrm{e}^{-a_2 x} + E_2'\mathrm{e}^{a_2 x},\ x\in(d,d+t], \\ E_3\cos(a_3 x + \Psi),\ x\in(d+t,d+t+h], \\ E_4\mathrm{e}^{-a_4 x},\ x\in(d+t+h,+\infty), \end{cases} \tag{6}$$

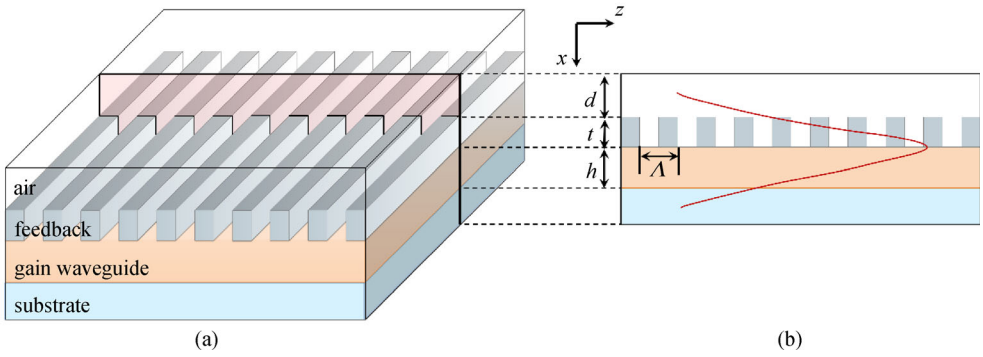

Fig. 7 (a) Schematic of DFB lasers; (b) reduced multi-layered model. Λ is the grating period; d is the thickness of air; t is the grating depth; h is the gain waveguide thickness. The red curve indicates the mode profile

here, k_z is the wave number in the z-direction. E_j and $E_2^{'}$ are the electric field amplitudes; a_j is the transverse wave number, and $a_j = \frac{2\pi}{\lambda}\sqrt{|n_{\text{eff}}^2 - n_j^2|}, j = 1, 2, 3, 4$; Ψ is a phase shift which is related with a_j. Ψ can be specified as $m\pi + \tan^{-1}\frac{a_4}{a_3} - (d + t + h)a_3$. m is a positive integer.

All electric field components can be calculated by applying the boundary condition. Therefore, the field distribution in each layer can be obtained [129,130]. By considering Eq. (1), the output wavelength can be also obtained.

Besides the couple wave theory, the photonic bandgap theory is also a full theory of DFB lasers [37,39,41]. The motivation comes from the fact that the resonant wavelength in Eq. (1) cannot propagate in the cavity due to the photonic bandgap. For easy understanding, a simplified model of 1D DFB lasers is derived using the coupled mode theory as follows. As shown in Fig. 7, the dielectric function of the cavity can be described by $\varepsilon(x,z) = \varepsilon^{(0)}(x) + \Delta\varepsilon(x,z)$. Here, $\varepsilon^{(0)}(x)$ is the dielectric function of the cavity without considering the grating; $\Delta\varepsilon(x,z)$ represents the periodic change of the dielectric function caused by the grating. Thus, the Fourier series of $\Delta\varepsilon(x,z)$ is described by

$$\Delta\varepsilon(x,z) = \varepsilon_0 \Sigma_{m\neq 0} \Delta\varepsilon_m(x) \mathrm{e}^{\mathrm{j}m\frac{2\pi}{\Lambda}z}, \tag{7}$$

here ε_0 is the dielectric constant in a vacuum. $\Delta\varepsilon_m(x)$ is the mth Fourier coefficients. The wave equation of TE modes (E_y component) can be derived as

$$\left[\frac{\partial^2}{\partial x^2} + \frac{\partial^2}{\partial z^2} + \omega^2\mu_0\varepsilon^{(0)}(x)\right]E_y = -\omega^2\mu_0\Delta\varepsilon(x,z)E_y, \tag{8}$$

where ω is the angular frequency, and μ_0 is the permeability in a vacuum. As mentioned above, there is a propagating waveguide mode ($A_+(z)$) and its counter-propagating waveguide mode ($A_-(z)$) in the cavity. The electric field distribution in the cavity is described as $[A_+(z)\mathrm{e}^{-\mathrm{j}\beta_z z} + A_-(z)\mathrm{e}^{\mathrm{j}\beta_z z}]E_y(x)$, where β_z denotes the wavevector in the z-direction. When $\beta_z = mG - \beta_z$, the two waveguide modes strongly coupled with each other. Here the grating vector is defined as $G = 2\pi/\Lambda$. Considering $\beta_z = 2\pi n_{\text{eff}}/\lambda_0$, the Bragg condition in Eq. (1) is obtained.

If we define the two waveguide modes as $a_+(z) = A_+(z)\mathrm{e}^{-\mathrm{j}\Delta\beta z}$ and $a_-(z) = A_-(z)\mathrm{e}^{\mathrm{j}\Delta\beta z}$, the coupled mode equation can be described as follows:

$$\frac{\partial}{\partial z}\begin{pmatrix} a_+(z) \\ a_-(z) \end{pmatrix} = -\mathrm{j}\begin{pmatrix} \Delta\beta & \kappa \\ -\kappa^* & -\Delta\beta \end{pmatrix}\begin{pmatrix} a_+(z) \\ a_-(z) \end{pmatrix}, \tag{9}$$

here $\beta_{\text{B}} = mG/2$, $\Delta\beta = \beta_z - \beta_{\text{B}}$, and κ is the coupling coefficient. By solving the eigenvalues of Eq. (9), the dispersion relationship of the resonant mode in the cavity is obtained as

$$\kappa = \beta_{\text{B}} \pm \sqrt{\Delta\beta^2 - |\kappa|^2}. \tag{10}$$

As shown in Eq. (10), the resonant wavelength satisfying the Bragg condition corresponds to the location of the photonic bandgap. Therefore, the photonic bandgap theory can predict the behavior of DFB lasers. For 2D and 3D cases, each photonic bandgap will affect the feedback due to the extended degree of freedom [36–38].

Special materials introduced in DFB lasers can also enrich the features, such as metallic materials [70,71,131], flexible materials [114,132,133], and fiber tips [134]. Take metallic materials as an example, plasmonics will improve the laser performance significantly by carefully designing [135–137]. Correspondingly, the related physical effect must be considered in the theoretical model [138,139].

3.3 Fabrication of laser cavities

One of the attractive advantages of DFB lasers based on organic materials is easy fabrication. A variety of fabrication schemes are used to introduce the organic materials in the DFB lasers, such as spin coating [140],

nanoimprint [141–143], nanograting transfer [144], thermal evaporation [144,145], horizontal dipping [146,147], ink-jet printing [148], and drop casting [149]. Note that the non-uniform film thickness should be considered in the last three methods. Recently, a versatile transfer coating method is proposed to assemble the DFB laser on arbitrary surfaces [80,134,150].

DFB cavities can be constructed by many approaches, such as interference lithography [44], nanoimprint lithography [151–153], photolithography [154], holographic interference [155–157], interference ablation [158,159], interference crosslinking [160,161], soft lithography [162], micromolding [147,163,164], electron beam lithography [165], and reactive ion etching [39].

The relative positions of the organic material, the DFB cavity, and the substrate are classified into three types, gain/cavity/substrate, cavity/gain/substrate, and active cavity/substrate, as shown in Fig. 8. There are some interesting differences in the laser performance of three configurations [44,107,159]. Based on the three configurations, complex cavities are designed to enrich the performance of DFB lasers, such as multilayer structures [130,140,166].

4 Advances in DFB laser based on organic materials

There are many excellent reviews dealing with the advances of DFB lasers based on organic materials [167–169]. In this paper, we will focus on some typical DFB lasers and the latest progress. These include new configurations, new fabrication methods, and performance improvements.

4.1 Lasing in 1D DFB cavities

As the most intuitive configuration, 1D DFB cavities has been investigated extensively. A variety of 1D structures are employed as DFB cavities, such as regular gratings [170], Fibonacci quasi-crystals [116], chirp gratings [35,171], beat gratings [172], and compound structures [108,109,173].

For 1D gratings, the output direction of the laser is related to the diffraction order followed Eq. (3). Therefore, edge-emitting lasers and surface-emitting lasers are achieved for the 1st order laser and the 2nd laser, respectively [174]. For high-order lasers, oblique emitting can be observed as shown in Fig. 9.

For DFB cavities based on Fibonacci quasi-crystals, the lasers exhibit some intriguing features, such as directional output independent of the emission frequency and multi-wavelength operation [116]. All the features can be controlled by engineering the self-similar spectrum of the grating structure. The multi-wavelength operation is a very attractive topic in the field of lasers, which can also be realized in 1D DFB cavities. The main features of DFB lasers with chirped gratings are the single mode operation and excellent tunability [171]. The laser pattern and number of wavelengths can be flexibly adjusted by the beat structures consisting of several parallel gratings [172]. The case of compound structures is subtly different, in such cavities, ultralow thresholds can be achieved by controlling over the balance between feedback and output coupling [108,173].

4.2 Lasing in 2D DFB cavities

For laser cavities based on 2D DFB structures, the feedback is more effective. Thus, the laser performance of 2D DFB lasers is much better than that of 1D cases, such as thresholds, wavelength numbers, laser modes/patterns, phase distributions, polarization, and beam divergence. Most 2D photonic crystals are used to realized DFB lasing, such as square lattices [111], rectangular lattices [175], triangular lattices [114], hexagonal lattices [38], quasi-crystals [176], fan-shaped gratings [119], circular structures [121], and spiral gratings [122].

Generally, the 2D DFB cavity provides complete 2D feedback due to the 2nd Bragg diffraction and acts simultaneously as an output coupler by the 1st Bragg diffraction. Similar to the 1D cases, the balance between feedback and coupling can be controlled by adjusting the cavity parameters. So, the laser performance is affected by the strength of the cavity coupling [110]. There are numerous intriguing features in lasers with 2D DFB cavities. The radial/azimuthal polarization of the output beam is controlled by the parameter of square lattices [177,178]. Multi-wavelength emissions can be easily realized in rectangular lattices and triangular lattices

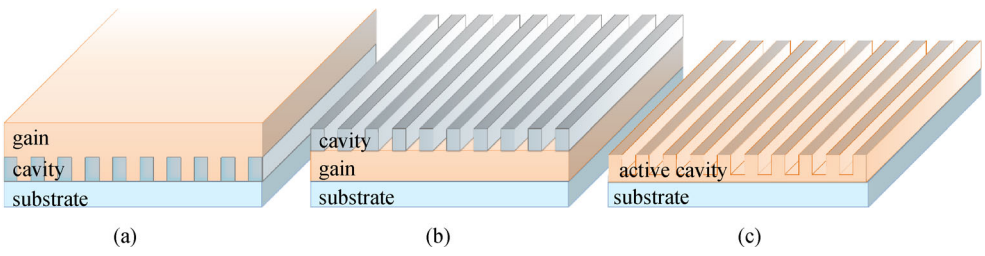

Fig. 8 Schematic of DFB lasers with different configurations. (a) Gain/cavity/substrate; (b) cavity/gain/substrate; (c) active cavity/substrate

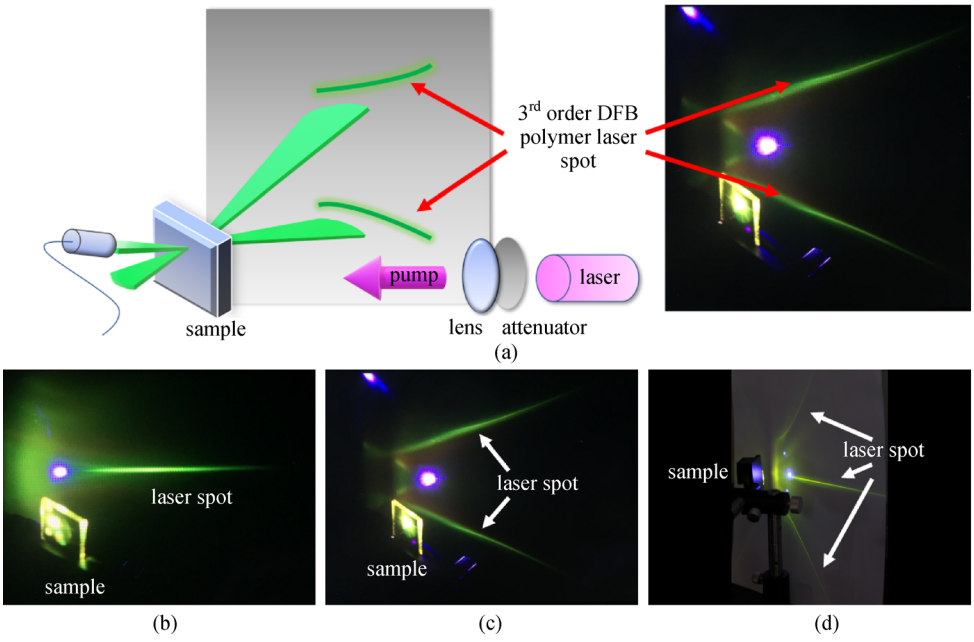

Fig. 9 (a) Illustration of the experimental setup and formation mechanism of the pattern of a 3rd order DFB polymer laser; the purple spots shown in the right photograph are the reflection and diffraction of the pumping laser; (b) 2nd order laser pattern; (c) 3rd order laser pattern; (d) 4th order laser pattern. Reproduced with permission [123]. Copyright 2019, MDPI

[114]. Even the continuously tunability over a wide spectral range is achieved in fan-shaped gratings [119]. For circular cavities, the beam divergence is very small (~10 mrad) due to the symmetry of the cavity [179].

From a wavefront manipulation point of view, the DFB cavity can modulate the phase distribution of the emission light. For a spiral grating as a DFB cavity, vortex lasers with desired topological charge can be obtained by completely controlling the phase, handedness, and degree of helicity of the emitted beam [122]. Figure 10 demonstrates the profiles of vortex lasers generated by spiral gratings.

4.3 Lasing in 3D DFB cavities

To date, relatively few studies have exploited the lasers based on 3D DFB cavities. The main reason is that most 3D photonic crystals are very difficult to be realized by micro-/nano-fabrication techniques. In this review, the 3D DFB cavities include 3D photonic crystals and stacked structures.

For 3D photonic crystals, lasing has been observed in holographic photonic crystals [154], liquid crystals [180], and opals photonic crystals [181,182]. In 3D photonic crystals, there exist many independent laser cavities which support multi-wavelength lasing emitted in different directions. Note that the symmetry of quasi-crystals is higher than that of periodic structures, which is easy to format photonic bandgaps. Therefore, the feedback for lasing is very efficient in quasi-crystals. Lasing has been observed in a 3D icosahedral quasicrystal fabricated by interference holography [183]. Multi-directional lasing is obtained due to the symmetry of quasi-crystals, as shown in Fig. 11.

The stacked structure consists of several 1D or 2D laser cavities [77,130,184]. Therefore, the laser properties of the stacked cavity are dependent on each component. For stacked structures, there are no 3D photonic bandgaps even considering the coupling effect.

4.4 Applications

As mentioned above, DFB cavities are the versatile building blocks for fundamental studies in nanoscale and potential applications. So far, many practical applications of organic DFB lasers have been proposed. One of the most straightforward applications is the visible light source integrated into spectroscopic systems. In particular, the lasers can be pumped by light-emitting diodes (LEDs) or laser diodes (LDs) [185,186], which accords with the trend of miniaturization of laser devices. It presents a versatile and powerful platform for various applications.

The broadly tunable emission throughout the visible range enables some applications in sensing [187–189], biomarker [190,191], high-performance light sources [192,193], on-chip communications [194,195], and optical circuits [196,197]. For example, label-free sensing can be achieved by a polymer DFB laser. The laser emission wavelength shifts with the variance of the effective refractive index modulated by the specific binding of the analyte [187]. Moreover, a lab-on-a-chip platform is constructed by integrating a 1st order organic DFB laser,

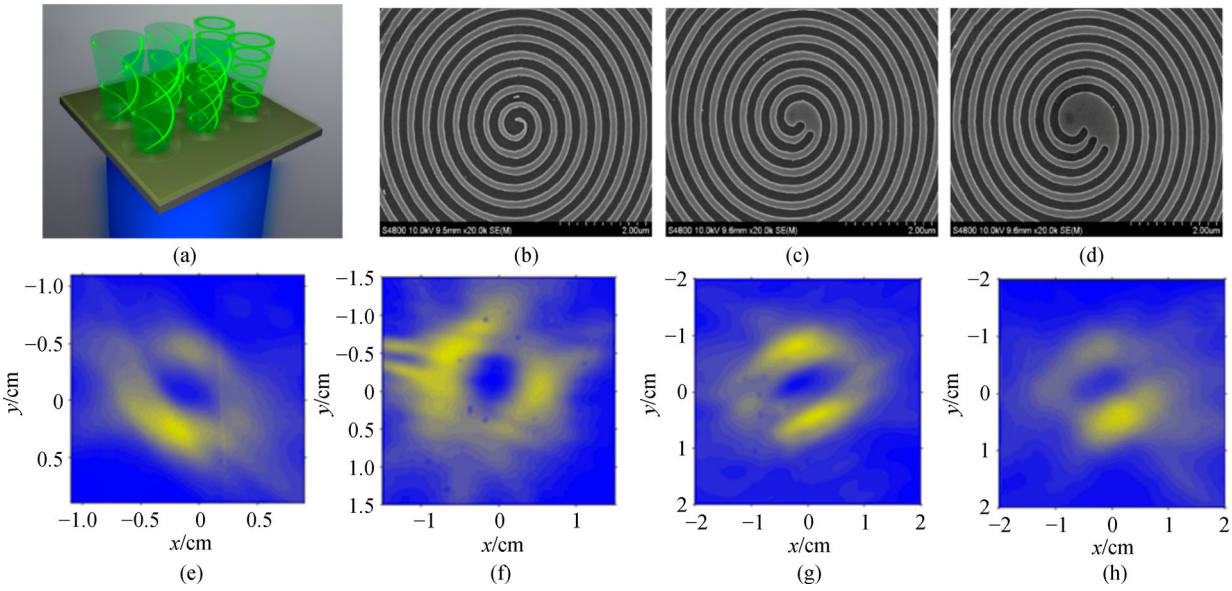

Fig. 10 (a) Schematic of organic vortex laser arrays based on spiral gratings. SEM images of the center of the (b) one-arm spiral, (c) two-arm spiral, and (d) three-arm spiral gratings. Beam profiles recorded for the beams generated using (e) circular, (f) one-arm, (g) two-arm, and (h) three-arm spiral gratings. Reproduced with permission [122]. Copyright 2018, ACS Publishing

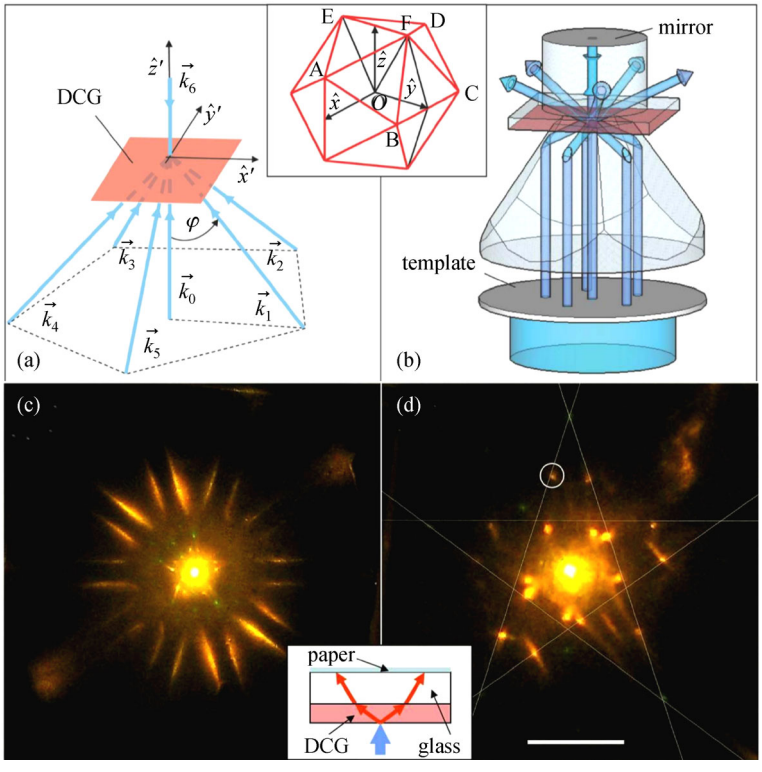

Fig. 11 (a) 7-beam configuration for the icosahedral quasicrystal. The upper inset denotes an icosahedral quasicrystal lattice; (b) actual 7-beam arrangement using a truncated pentagonal pyramid; (c) icosahedral quasicrystal lasing pattern projected on the back side of the glass substrate (see lower inset). DCG is the abbreviation of the dichromate gelatin emulsions; (d) higher resolution projection of the icosahedral quasicrystal lasing for inner region. The lines are guides to the eyes. Reproduced with permission [183]. Copyright 2009, OSA Publishing

deep ultraviolet induced waveguides, and a nanostructured microfluidic channel into a poly (methyl methacrylate) substrate.

5 Summary and outlook

In summary, DFB lasing in photonic crystals has been extensively investigated in the past three decades. Numerous exciting developments have taken place in the field of DFB lasers based on organic materials. However, from the applications-based research point of view, there exist two limitations which baffle the marketization of such laser devices.

The first limitation is miniaturization. One the one hand, the size of the optical pump source is too large to integrate; on the other hand, the electrical pumping laser remains one of the major challenges. The challenges to be overcome include the excited-state triplet absorption, the absorption of metal contacts, and current densities required. In fact, organic semiconductors have some intrinsic drawbacks, such as low mobility and accumulated triplet states. The settlements may require significant innovations in materials science and engineering. Two feasible strategies for a trade-off between optical pumping and electrical pumping are indirect electrical pumping and fiber-based design. For indirect electrical pumping, the electrically driven light source (LEDs or LDs) is used to pump the organic semiconductor DFB laser optically. For the fiber-based design, the organic semiconductor DFB laser is fabricated on the fiber facet, removing the restriction of the electrical pumping.

The second limitation is the performance problems. Compared with commercial lasers, the output energy of the organic semiconductor DFB laser is relatively low, which is attributed to the small excitation volume. The continuous wave lasing is difficult to achieve in regular configurations. In most cases, pulsed wave lasing is obtained due to the long-lived triplet states. Moreover, some significant issues remain largely unexplored, such as the frequency repetition, pulse width, stability of materials, and lifetime of devices. Up to now, there are few researches involving the laser modulated techniques of organic semiconductor DFB lasers, including property manipulations and loading information. These techniques relate to amplitude modulation, intensity modulation, and phase modulation. Specific means include the *Q*-switching, mode locking, and so on. Further investigation is required to overcome the limitations to significantly enhance the laser performance. New opportunities and further progress can be expected from developing materials and techniques specifically for organic semiconductor DFB lasers.

Acknowledgements This work was supported by the National Natural Science Foundation of China (Grant Nos. 61822501, 11734001, and 11704017) and the Beijing Natural Science Foundation (No. Z180015).

References

1. Yablonovitch E. Inhibited spontaneous emission in solid-state physics and electronics. Physical Review Letters, 1987, 58(20): 2059–2062
2. John S. Strong localization of photons in certain disordered dielectric superlattices. Physical Review Letters, 1987, 58(23): 2486–2489
3. Joannopoulos J D, Villeneuve P R, Fan S. Photonic crystals: putting a new twist on light. Nature, 1997, 386(6621): 143–149
4. Sakoda K. Optical Properties of Photonic Crystals. New York: Springer, 2001
5. Zhai T, Liu D, Zhang X. Photonic crystals and microlasers fabricated with low refractive index material. Frontiers in Physics, 2010, 5(3): 266–276
6. Krauss T F, Rue R, Brand S. Two-dimensional photonic-bandgap structures operating at near-infrared wavelengths. Nature, 1996, 383(6602): 699–702
7. Zoorob M E, Charlton M D, Parker G J, Baumberg J J, Netti M C. Complete photonic bandgaps in 12-fold symmetric quasicrystals. Nature, 2000, 404(6779): 740–743
8. Campbell M, Sharp D N, Harrison M T, Denning R G, Turberfield A J. Fabrication of photonic crystals for the visible spectrum by holographic lithography. Nature, 2000, 404(6773): 53–56
9. Bendickson J M, Dowling J P, Scalora M. Analytic expressions for the electromagnetic mode density in finite, one-dimensional, photonic band-gap structures. Physical Review E, 1996, 53(4): 4107–4121
10. Boedecker G, Henkel C. All-frequency effective medium theory of a photonic crystal. Optics Express, 2003, 11(13): 1590–1595
11. Wang Z, Zhai T, Lin J, Liu D. Effect of surface truncation on mode density in photonic crystals. Journal of the Optical Society of America B, Optical Physics, 2007, 24(9): 2416–2420
12. Dowling J, Scalora M, Bloemer M, Bowden C. The photonic band edge laser: a new approach to gain enhancement. Journal of Applied Physics, 1994, 75(4): 1896–1899
13. Cho C O, Jeong J, Lee J, Jeon H, Kim I, Jang D H, Park Y S, Woo J C. Photonic crystal band edge laser array with a holographically generated square-lattice pattern. Applied Physics Letters, 2005, 87 (16): 161102
14. Kim H, Lee M, Jeong H, Hwang M S, Kim H R, Park S, Park Y D, Lee T, Park H G, Jeon H. Electrical modulation of a photonic crystal band-edge laser with a graphene monolayer. Nanoscale, 2018, 10(18): 8496–8502
15. Hu X, Jiang P, Ding C, Yang H, Gong Q. Picosecond and low-power all-optical switching based on an organic photonic-bandgap microcavity. Nature Photonics, 2008, 2(3): 185–189
16. Bose R, Sridharan D, Kim H, Solomon G S, Waks E. Low-photon-number optical switching with a single quantum dot coupled to a photonic crystal cavity. Physical Review Letters, 2012, 108(22): 227402
17. Nozaki K, Shinya A, Matsuo S, Sato T, Kuramochi E, Notomi M. Ultralow-energy and high-contrast all-optical switch involving Fano resonance based on coupled photonic crystal nanocavities. Optics Express, 2013, 21(10): 11877–11888

18. Liu Q, Ouyang Z, Wu C J, Liu C P, Wang J C. All-optical half adder based on cross structures in two-dimensional photonic crystals. Optics Express, 2008, 16(23): 18992–19000
19. McCutcheon M W, Rieger G W, Young J F, Dalacu D, Poole P J, Williams R L. All-optical conditional logic with a nonlinear photonic crystal nanocavity. Applied Physics Letters, 2009, 95 (22): 221102
20. Fu Y, Hu X, Gong Q. Silicon photonic crystal all-optical logic gates. Physics Letters A, 2013, 377(3–4): 329–333
21. Rupasov V I V I, Singh M. Quantum gap solitons and many-polariton-atom bound states in dispersive medium and photonic band gap. Physical Review Letters, 1996, 77(2): 338–341
22. Xie P, Zhang Z Q. Multifrequency gap solitons in nonlinear photonic crystals. Physical Review Letters, 2003, 91(21): 213904
23. Peleg O, Bartal G, Freedman B, Manela O, Segev M, Christodoulides D N. Conical diffraction and gap solitons in honeycomb photonic lattices. Physical Review Letters, 2007, 98 (10): 103901
24. Wu J, Day D, Gu M. A microfluidic refractive index sensor based on an integrated three-dimensional photonic crystal. Applied Physics Letters, 2008, 92(7): 071108
25. Kang C, Phare C T, Vlasov Y A, Assefa S, Weiss S M. Photonic crystal slab sensor with enhanced surface area. Optics Express, 2010, 18(26): 27930–27937
26. Sørensen K T, Ingvorsen C B, Nielsen L H, Kristensen A. Effects of water-absorption and thermal drift on a polymeric photonic crystal slab sensor. Optics Express, 2018, 26(5): 5416–5422
27. Painter O, Lee R K, Scherer A, Yariv A, O'Brien J D, Dapkus P D, Kim I. Two-dimensional photonic band-gap defect mode laser. Science, 1999, 284(5421): 1819–1821
28. Park H G, Kim S H, Kwon S H, Ju Y G, Yang J K, Baek J H, Kim S B, Lee Y H. Electrically driven single-cell photonic crystal laser. Science, 2004, 305(5689): 1444–1447
29. Yang X, Wong C W. Coupled-mode theory for stimulated Raman scattering in high-Q/V_{m} silicon photonic band gap defect cavity lasers. Optics Express, 2007, 15(8): 4763–4780
30. Ryu H Y, Kwon S H, Lee Y J, Lee Y H, Kim F. Very low threshold photonic band edge lasers from free standing trlangular photonic crystal slabs. Applied Physics Letters, 2002, 80(19): 3476–3478
31. Arango F B, Christiansen M B, Gersborg-Hansen M, Kristensen A. Optofluidic tuning of photonic crystal band edge lasers. Applied Physics Letters, 2007, 91(22): 223503
32. Jung H, Lee M, Han C, Park Y, Cho K S, Jeon H. Efficient on-chip integration of a colloidal quantum dot photonic crystal band-edge laser with a coplanar waveguide. Optics Express, 2017, 25(26): 32919
33. Monat C, Seassal C, Letartre X, Regreny P, Rojo-Romeo P, Viktorovitch P, Le Vassor d'Yerville M, Cassagne D, Albert J P, Jalaguier E, Pocas S, Aspar B. InP-based two-dimensional photonic crystal on silicon: in-plane Bloch mode laser. Applied Physics Letters, 2002, 81(27): 5102–5104
34. Imada M, Noda S, Chutinan A, Tokuda T, Murata M, Sasaki G. Coherent two-dimensional lasing action in surface-emitting laser with triangular-lattice photonic crystal structure. Applied Physics Letters, 1999, 75(3): 316–318
35. Kok M, Lu W, Lee J, Tam W, Wong G, Chan C. Lasing from dye-doped photonic crystals with graded layers in dichromate gelatin emulsions. Applied Physics Letters, 2008, 92(15): 151108
36. Meier M, Mekis A, Dodabalapur A, Timko A, Slusher R E, Joannopoulos J D, Nalamasu O. Laser action from two-dimensional distributed feedback in photonic crystals. Applied Physics Letters, 1999, 74(1): 7–9
37. Riechel S, Kallinger C, Lemmer U, Feldmann J, Gombert A, Wittwer V, Scherf U. A nearly diffraction limited surface emitting conjugated polymer laser utilizing a two-dimensional photonic band structure. Applied Physics Letters, 2000, 77(15): 2310–2312
38. Notomi M, Suzuki H, Tamamura T. Directional lasing oscillation of two-dimensional organic photonic crystal lasers at several photonic band gaps. Applied Physics Letters, 2001, 78(10): 1325–1327
39. Turnbull G, Andrew P, Jory M, Barnes W L, Samuel I. Relationship between photonic band structure and emission characteristics of a polymer distributed feedback laser. Physical Review B, 2001, 64(12): 125122
40. Andrew P, Turnbull G, Samuel I, Barnes W. Photonic band structure and emission characteristics of a metal-backed polymeric distributed feedback laser. Applied Physics Letters, 2002, 81(6): 954–956
41. Turnbull G, Andrew P, Barnes W L, Samuel I. Photonic mode dispersion of a two-dimensional distributed feedback polymer laser. Physical Review B, 2003, 67(16): 165107
42. Samuel I D, Turnbull G A. Polymer lasers: recent advances. Materials Today, 2004, 7(9): 28–35
43. Herrnsdorf J, Guilhabert B, Chen Y, Kanibolotsky A, Mackintosh A, Pethrick R, Skabara P, Gu E, Laurand N, Dawson M. Flexible blue-emitting encapsulated organic semiconductor DFB laser. Optics Express, 2010, 18(25): 25535–25545
44. Zhai T, Zhang X, Pang Z. Polymer laser based on active waveguide grating structures. Optics Express, 2011, 19(7): 6487–6492
45. Vecchi G, Raineri F, Sagnes I, Yacomotti A, Monnier P, Karle T J, Lee K H, Braive R, Le Gratiet L, Guilet S, Beaudoin G, Taneau A, Bouchoule S, Levenson A, Raj R. Continuous-wave operation of photonic band-edge laser near 1.55 μm on silicon wafer. Optics Express, 2007, 15(12): 7551–7556
46. Van der Ziel J P, Tsang W T, Logan R A, Mikulyak R M, Augustyniak W M. Subpicosecond pulses from passively mode-locked GaAs buried optical guide semiconductor lasers. Applied Physics Letters, 1981, 39(7): 525–527
47. Dahmani B, Hollberg L, Drullinger R. Frequency stabilization of semiconductor lasers by resonant optical feedback. Optics Letters, 1987, 12(11): 876–878
48. San Miguel M, Feng Q, Moloney J V. Light-polarization dynamics in surface-emitting semiconductor lasers. Physical Review A, 1995, 52(2): 1728–1739
49. Shank C V. Physics of dye lasers. Reviews of Modern Physics, 1975, 47(3): 649–657
50. Ledentsov N N, Ustinov V M, Egorov A Y, Zhukov A E, Maksimov M V, Tabatadze I G, Kop'ev P S. Optical properties of heterostructures with InGaAs-GaAs quantum clusters. Semiconductors, 1994, 28(8): 832–834
51. Kirstaedter N, Schmidt O G, Ledentsov N N, Bimberg D, Ustinov V M, Egorov A Y, Zhukov A E, Maximov M V, Kop'ev P S,

Alferov Z I. Gain and differential gain of single layer InAs/GaAs quantum dot injection lasers. Applied Physics Letters, 1996, 69(9): 1226–1228
52. Bimberg D, Grundmann M, Heinrichsdorff F, Ledentsov N N, Ustinov V M, Zhukov A E, Kovsh A R, Maximov M V, Shernyakov Y M, Volovik B V, Tsatsul'nikov A F, Kop'ev P S, Alferov Z I. Quantum dot lasers: breakthrough in optoelectronics. Thin Solid Films, 2000, 367(1–2): 235–249
53. Veldhuis S A, Boix P P, Yantara N, Li M, Sum T C, Mathews N, Mhaisalkar S G. Perovskite materials for light-emitting diodes and lasers. Advanced Materials, 2016, 28(32): 6804–6834
54. Wang K, Wang S, Xiao S, Song Q. Recent advances in perovskite micro- and nanolasers. Advanced Optical Materials, 2018, 6(18): 1800278
55. Wei Q, Li X, Liang C, Zhang Z, Guo J, Hong G, Xing G, Huang W. Recent progress in metal halide perovskite micro- and nanolasers. Advanced Optical Materials, 2019, 7(20): 1900080
56. Zhang W F, Zhu H, Yu S F, Yang H Y. Observation of lasing emission from carbon nanodots in organic solvents. Advanced Materials, 2012, 24(17): 2263–2267
57. Qu S, Liu X, Guo X, Chu M, Zhang L, Shen D. Amplified spontaneous green emission and lasing emission from carbon nanoparticles. Advanced Functional Materials, 2014, 24(18): 2689–2695
58. Tang C W, Vanslyke S A. Organic electroluminescent diodes. Applied Physics Letters, 1987, 51(12): 913–915
59. Schön J H, Kloc C, Dodabalapur A, Batlogg B. An organic solid state injection laser. Science, 2000, 289(5479): 599–601
60. Montes V A, Li G, Pohl R, Shinar J, Anzenbacher P. Effective color tuning in organic light-emitting diodes based on aluminum Tris(5-aryl-8-hydroxyquinoline) complexes. Advanced Materials, 2004, 16(22): 2001–2003
61. Lawrence J R, Turnbull G A, Samuel I D, Richards G J, Burn P L. Optical amplification in a first-generation dendritic organic semiconductor. Optics Letters, 2004, 29(8): 869–871
62. Spehr T, Siebert A, Fuhrmann-Lieker T, Salbeck J, Rabe T, Riedl T, Johannes H H, Kowalsky W, Wang J, Weimann T, Hinze P. Organic solid-state ultraviolet-laser based on spiro-terphenyl. Applied Physics Letters, 2005, 87(16): 161103
63. Xia R, Lai W Y, Levermore P A, Huang W, Bradley D D C. Low-threshold distributed-feedback lasers based on Pyrene-cored starburst molecules with 1,3,6,8-attached Oligo(9,9-Dialkylfluorene) arms. Advanced Functional Materials, 2009, 19(17): 2844–2850
64. Tessler N, Denton G, Friend R. Lasing from conjugated-polymer microcavities. Nature, 1996, 382(6593): 695–697
65. Campoy-Quiles M, Heliotis G, Xia R, Ariu M, Pintani M, Etchegoin P, Bradley D D C. Ellipsometric characterization of the optical constants of polyfluorene gain media. Advanced Functional Materials, 2005, 15(6): 925–933
66. Yap B K, Xia R, Campoy-Quiles M, Stavrinou P N, Bradley D D C. Simultaneous optimization of charge-carrier mobility and optical gain in semiconducting polymer films. Nature Materials, 2008, 7(5): 376–380
67. Lawrence J R, Turnbull G A, Samuel I D W. Polymer laser fabricated by a simple micromolding process. Applied Physics Letters, 2003, 82(23): 4023–4025
68. Goossens M, Ruseckas A, Turnbull G A, Samuel I D W. Subpicosecond pulses from a gain-switched polymer distributed feedback laser. Applied Physics Letters, 2004, 85(1): 31–33
69. O'Neill M, Kelly S M. Ordered materials for organic electronics and photonics. Advanced Materials, 2011, 23(5): 566–584
70. Stehr J, Crewett J, Schindler F, Sperling R, von Plessen G, Lemmer U, Lupton J M, Klar T A, Feldmann J, Holleitner A W, Forster M, Scherf U. A low threshold polymer laser based on metallic nanoparticle gratings. Advanced Materials, 2003, 15(20): 1726–1729
71. Reufer M, Riechel S, Lupton J, Feldmann J, Lemmer U, Schneider D, Benstem T, Dobbertin T, Kowalsky W, Gombert A, Forberich K, Wittwer V, Scherf U. Low-threshold polymeric distributed feedback lasers with metallic contacts. Applied Physics Letters, 2004, 84(17): 3262–3264
72. Marcus M, Milward J D, Köhler A, Barford W. Structural information for conjugated polymers from optical modeling. Journal of Physical Chemistry A, 2018, 122(14): 3621–3625
73. Virgili T, Lidzey D G, Grell M, Bradley D D C, Stagira S, Zavelani-Rossi M, De Silvestri S. Influence of the orientation of liquid crystalline poly(9,9-dioctylfluorene) on its lasing properties in a planar microcavity. Applied Physics Letters, 2002, 80(22): 4088–4090
74. Yang Y, Turnbull G A, Samuel I D W. Sensitive explosive vapor detection with polyfluorene lasers. Advanced Functional Materials, 2010, 20(13): 2093–2097
75. Giovanella U, Betti P, Bolognesi A, Destri S, Melucci M, Pasini M, Porzio W, Botta C. Core-type polyfluorene-based copolymers for low-cost light-emitting technologies. Organic Electronics, 2010, 11(12): 2012–2018
76. Yan M, Rothberg L J, Papadimitrakopoulos F, Galvin M E, Miller T M. Spatially indirect excitons as primary photoexcitations in conjugated polymers. Physical Review Letters, 1994, 72(7): 1104–1107
77. Heliotis G, Bradley D D C, Turnbull G A, Samuel I D W. Light amplification and gain in polyfluorene waveguides. Applied Physics Letters, 2002, 81(3): 415–417
78. Chang S J, Liu X, Lu T T, Liu Y Y, Pan J Q, Jiang Y, Chu S Q, Lai W Y, Huang W. Ladder-type poly(indenofluorene-co-benzothiadiazole)s as efficient gain media for organic lasers: design, synthesis, optical gain properties, and stabilized lasing properties. Journal of Materials Chemistry C, Materials for Optical and Electronic Devices, 2017, 5(26): 6629–6639
79. Lahoz F, Capuj N, Oton C J, Cheylan S. Optical gain in conjugated polymer hybrid structures based on porous silicon waveguides. Chemical Physics Letters, 2008, 463(4–6): 387–390
80. Zhai T, Wang Y, Chen L, Wu X, Li S, Zhang X. Red-green-blue laser emission from cascaded polymer membranes. Nanoscale, 2015, 7(47): 19935–19939
81. Sorokin P P, Lankard J R. Stimulated emission observed from an organic dye, chloro-aluminum phthalocyanine. IBM Journal of Research and Development, 1966, 10(2): 162–163
82. Czerney P, Graneß G, Birckner E, Vollmer F, Rettig W. Molecular engineering of cyanine-type fluorescent and laser dyes. Journal of Photochemistry and Photobiology A Chemistry, 1995, 89(1): 31–

36
83. Khairutdinov R F, Serpone N. Photophysics of cyanine dyes: subnanosecond relaxation dynamics in monomers, dimers, and H- and J-aggregates in solution. Journal of Physical Chemistry B, 1997, 101(14): 2602–2610
84. Cerdán L, Costela A, Garcíamoreno I, Bañuelos J, Lópezarbeloa I. Singular laser behavior of hemicyanine dyes: unsurpassed efficiency and finely structured spectrum in the near-IR region. Laser Physics Letters, 2012, 9(6): 426–433
85. Tomasulo M, Sortino S, White A J P, Raymo F M. Fast and stable photochromic oxazines. Journal of Organic Chemistry, 2005, 70 (20): 8180–8189
86. Shi X, Wang Y, Wang Z, Sun Y, Liu D, Zhang Y, Li Q, Shi J. High performance plasmonic random laser based on nanogaps in bimetallic porous nanowires. Applied Physics Letters, 2013, 103 (2): 023504
87. Zhai T, Wang Y, Liu H, Zhang X. Large-scale fabrication of flexible metallic nanostructure pairs using interference ablation. Optics Express, 2015, 23(2): 1863–1870
88. Jones G II, Jackson W, Halpern A. Medium effects on fluorescence quantum yields and lifetimes for coumarin laser dyes. Chemical Physics Letters, 1980, 72(2): 391–395
89. Liu X, Cole J M, Waddell P G, Lin T C, Radia J, Zeidler A. Molecular origins of optoelectronic properties in coumarin dyes: toward designer solar cell and laser applications. Journal of Physical Chemistry A, 2012, 116(1): 727–737
90. Wang Y, Shi X, Sun Y, Zheng R, Wei S, Shi J, Wang Z, Liu D. Cascade-pumped random lasers with coherent emission formed by Ag-Au porous nanowires. Optics Letters, 2014, 39(1): 5–8
91. Wong M M, Schelly Z A. Solvent-jump relaxation kinetics of the association of Rhodamine type laser dyes. Journal of Physical Chemistry, 1974, 78(19): 1891–1895
92. Zhai T, Zhou Y, Chen S, Wang Z, Shi J, Liu D, Zhang X. Pulse-duration-dependent and temperature-tunable random lasing in a weakly scattering structure formed by speckles. Physical Review A., 2010, 82(2): 023824
93. Zhai T, Chen J, Chen L, Wang J, Wang L, Liu D, Li S, Liu H, Zhang X. A plasmonic random laser tunable through stretching silver nanowires embedded in a flexible substrate. Nanoscale, 2015, 7(6): 2235–2240
94. Kan S C, Vassilovski D, Wu T C, Lau K Y. Quantum capture limited modulation bandwidth of quantum well, wire, and dot lasers. Applied Physics Letters, 1993, 62(19): 2307–2309
95. Kirstaedter N, Ledentsov N N, Grundmann M, Bimberg D, Ustinov V M, Ruvimov S S, MaximovM V, Kop′ev P S, Alferov Z I, Richter U, Werner P, Gösele U, Heydenreich J. Low threshold, large T_0 injection laser emission from (InGa)As quantum dots. Electronics Letters, 1994, 30(17): 1416–1417
96. Fafard S, Hinzer K, Raymond S, Dion M, McCaffrey J, Feng Y, Charbonneau S. Red-emitting semiconductor quantum dot lasers. Science, 1996, 274(5291): 1350–1353
97. Yamashita K, Kitanobou A, Ito M, Fukuzawa E, Oe K. Solid-state organic laser using self-written active waveguide with in-line Fabry–Pérot cavity. Applied Physics Letters, 2008, 92(14): 143305
98. Yamashita K, Yanagi H, Oe K. Array of a dye-doped polymer-based microlaser with multiwavelength emission. Optics Letters, 2011, 36(10): 1875–1877
99. Lafargue C, Bittner S, Lozenko S, Lautru J, Zyss J, Ulysse C, Cluzel C, Lebental M. Three-dimensional emission from organic Fabry-Perot microlasers. Applied Physics Letters, 2013, 102(25): 251120
100. Frolov S, Shkunov M, Vardeny Z, Yoshino K. Ring microlasers from conducting polymers. Physical Review B, 1997, 56(8): 4363–4366
101. Frolov S V, Vardeny Z V, Yoshino K. Plastic microring lasers on fibers and wires. Applied Physics Letters, 1998, 72(15): 1802–1804
102. Kushida S, Okada D, Sasaki F, Lin Z H, Huang J S, Yamamoto Y. Lasers: low-threshold whispering gallery mode lasing from self-assembled microspheres of single-sort conjugated polymers. Advanced Optical Materials, 2017, 5(10): 1700123
103. Persano L, Camposeo A, Del Carro P, Mele E, Cingolani R, Pisignano D. Very high-quality distributed Bragg reflectors for organic lasing applications by reactive electron-beam deposition. Optics Express, 2006, 14(5): 1951–1956
104. Singer K D, Kazmierczak T, Lott J, Song H, Wu Y, Andrews J, Baer E, Hiltner A, Weder C. Melt-processed all-polymer distributed Bragg reflector laser. Optics Express, 2008, 16(14): 10358–10363
105. Tsutsumi N, Ishibashi T. Organic dye lasers with distributed Bragg reflector grating and distributed feedback resonator. Optics Express, 2009, 17(24): 21698–21703
106. Kretsch K P, Blau W J, Dumarcher V, Rocha L, Fiorini C, Nunzi J M, Pfeiffer S, Tillmann H, Hörhold H H. Distributed feedback laser action from polymeric waveguides doped with oligo phenylene vinylene model compounds. Applied Physics Letters, 2000, 76 (16): 2149–2151
107. Zhai T R, Zhang X P, Dou F. Microscopic excavation into the optically pumped polymer lasers based on distributed feedback. Chinese Physics Letters, 2012, 29(10): 104204
108. Martins E R, Wang Y, Kanibolotsky A L, Skabara P J, Turnbull G A, Samuel I D. Low-threshold nanoimprinted lasers using substructured gratings for control of distributed feedback. Advanced Optical Materials, 2013, 1(8): 563–566
109. Zhai T, Wu X, Li S, Liang S, Niu L, Wang M, Feng S, Liu H, Zhang X. Polymer lasing in a periodic-random compound cavity. Polymers, 2018, 10(11): 1194
110. Zhang S, Tong J, Chen C, Cao F, Liang C, Song Y, Zhai T, Zhang X. Controlling the performance of polymer lasers via the cavity coupling. Polymers, 2019, 11(5): 764
111. Heliotis G, Xia R, Turnbull G, Andrew P, Barnes W L, Samuel I D W, Bradley D D C. Emission characteristics and performance comparison of polyfluorene lasers with one-and two-dimensional distributed feedback. Advanced Functional Materials, 2004, 14(1): 91–97
112. Cao H, Zhao Y, Ho S, Seelig E, Wang Q, Chang R. Random laser action in semiconductor powder. Physical Review Letters, 1999, 82(11): 2278–2281
113. Wiersma D. The physics and applications of random lasers. Nature Physics, 2008, 4(5): 359–367
114. Zhai T, Wang Y, Chen L, Zhang X. Direct writing of tunable multi-wavelength polymer lasers on a flexible substrate. Nanoscale,

2015, 7(29): 12312–12317
115. Deotare P B, Mahony T S, Bulović V. Ultracompact low-threshold organic laser. ACS Nano, 2014, 8(11): 11080–11085
116. Mahler L, Tredicucci A, Beltram F, Walther C, Faist J, Beere H E, Ritchie D A, Wiersma D S. Quasi-periodic distributed feedback laser. Nature Photonics, 2010, 4(3): 165–169
117. Man W, Megens M, Steinhardt P J, Chaikin P M. Experimental measurement of the photonic properties of icosahedral quasicrystals. Nature, 2005, 436(7053): 993–996
118. Vardeny Z V, Nahata A, Agrawal A. Optics of photonic quasicrystals. Nature Photonics, 2013, 7(3): 177–187
119. Zhai T, Cao F, Chu S, Gong Q, Zhang X. Continuously tunable distributed feedback polymer laser. Optics Express, 2018, 26(4): 4491–4497
120. Barlow G, Shore K. Threshold gain and threshold current analysis of circular grating DFB organic semiconductor lasers. IEE Proceedings-Optoelectronics, 2001, 148(4): 165–170
121. Bauer C, Giessen H, Schnabel B, Kley E B, Schmitt C, Scherf U, Mahrt R F. A surface-emitting circular grating polymer laser. Advanced Materials, 2001, 13(15): 1161–1164
122. Stellinga D, Pietrzyk M E, Glackin J M E, Wang Y, Bansal A K, Turnbull G A, Dholakia K, Samuel I D W, Krauss T F. An organic vortex laser. ACS Nano, 2018, 12(3): 2389–2394
123. Zhou P, Niu L, Hayat A, Cao F, Zhai T, Zhang X. Operating characteristics of high-order distributed feedback polymer lasers. Polymers, 2019, 11(2): 258
124. Zhai T, Zhang X. Gain- and feedback-channel matching in lasers based on radiative-waveguide gratings. Applied Physics Letters, 2012, 101(14): 143507
125. Kogelnik H, Shank C V. Coupled-wave theory of distributed feedback lasers. Journal of Applied Physics, 1972, 43(5): 2327–2335
126. Kazarinov R F, Henry C H. Second-order distributed feedback lasers with mode selection provided by first-order radiation losses. IEEE Journal of Quantum Electronics, 1985, 21(2): 144–150
127. Scheuer J, Yariv A. Coupled-waves approach to the design and analysis of Bragg and photonic crystal annular resonators. IEEE Journal of Quantum Electronics, 2003, 39(12): 1555–1562
128. Vannahme C, Smith C L C, Christiansen M B, Kristensen A. Emission wavelength of multilayer distributed feedback dye lasers. Applied Physics Letters, 2012, 101(15): 151123
129. Huang W, Shen S, Pu D, Wei G, Ye Y, Peng C, Chen L. Working characteristics of external distributed feedback polymer lasers with varying waveguiding structures. Journal of Physics D, 2015, 48 (49): 495105
130. Zhai T, Wu X, Wang M, Tong F, Li S, Ma Y, Deng J, Zhang X. Dual-wavelength polymer laser based on an active/inactive/active sandwich-like structure. Applied Physics Letters, 2016, 109(10): 101906
131. Van Beijnum F, Van Veldhoven P J, Geluk E J, De Dood M J A, 't Hooft G W, Van Exter M P. Surface plasmon lasing observed in metal hole arrays. Physical Review Letters, 2013, 110(20): 206802
132. Kallinger C, Hilmer M, Haugeneder A, Perner M, Spirkl W, Lemmer U, Feldmann J, Scherf U, Müllen K, Gombert A, Wittwer V. A flexible conjugated polymer laser. Advanced Materials, 1998, 10(12): 920–923
133. Wenger B, Tétreault N, Welland M, Friend R. Mechanically tunable conjugated polymer distributed feedback lasers. Applied Physics Letters, 2010, 97(19): 193303
134. Zhai T, Chen L, Li S, Hu Y, Wang Y, Wang L, Zhang X. Free-standing membrane polymer laser on the end of an optical fiber. Applied Physics Letters, 2016, 108(4): 041904
135. Chen C, Tong F, Cao F, Tong J, Zhai T, Zhang X. Tunable polymer lasers based on metal-dielectric hybrid cavity. Optics Express, 2018, 26(24): 32048–32054
136. Cao F, Niu L, Tong J, Li S, Hayat A, Wang M, Zhai T, Zhang X. Hybrid lasing in a plasmonic cavity. Optics Express, 2018, 26(10): 13383–13389
137. Zhai T, Tong F, Cao F, Niu L, Li S, Wang M, Zhang X. Distributed feedback lasing in a metallic cavity. Applied Physics Letters, 2017, 111(11): 111901
138. Andrew P, Turnbull G A, Samuel I D, Barnes W L. Photonic band structure and emission characteristics of a metal-backed polymeric distributed feedback laser. Applied Physics Letters, 2002, 81(6): 954–956
139. Zhou W, Dridi M, Suh J Y, Kim C H, Co D T, Wasielewski M R, Schatz G C, Odom T W. Lasing action in strongly coupled plasmonic nanocavity arrays. Nature Nanotechnology, 2013, 8(7): 506–511
140. Foucher C, Guilhabert B, Kanibolotsky A L, Skabara P J, Laurand N, Dawson M D. RGB and white-emitting organic lasers on flexible glass. Optics Express, 2016, 24(3): 2273–2280
141. Wang Y, Tsiminis G, Kanibolotsky A L, Skabara P J, Samuel I D, Turnbull G A. Nanoimprinted polymer lasers with threshold below 100 W/cm^2 using mixed-order distributed feedback resonators. Optics Express, 2013, 21(12): 14362–14367
142. Whitworth G L, Zhang S, Stevenson J R Y, Ebenhoch B, Samuel I D W, Turnbull G A. Solvent immersion nanoimprint lithography of fluorescent conjugated polymers. Applied Physics Letters, 2015, 107(16): 163301
143. Gaal M, Gadermaier C, Plank H, Moderegger E, Pogantsch A, Leising G, List E J W. Imprinted conjugated polymer laser. Advanced Materials, 2003, 15(14): 1165–1167
144. Liu X, Klinkhammer S, Wang Z, Wienhold T, Vannahme C, Jakobs P J, Bacher A, Muslija A, Mappes T, Lemmer U. Pump spot size dependent lasing threshold in organic semiconductor DFB lasers fabricated via nanograting transfer. Optics Express, 2013, 21(23): 27697–27706
145. Baldo M, Deutsch M, Burrows P, Gossenberger H, Gerstenberg M, Ban V, Forrest S. Organic vapor phase deposition. Advanced Materials, 1998, 10(18): 1505–1514
146. Klinkhammer S, Liu X, Huska K, Shen Y, Vanderheiden S, Valouch S, Vannahme C, Bräse S, Mappes T, Lemmer U. Continuously tunable solution-processed organic semiconductor DFB lasers pumped by laser diode. Optics Express, 2012, 20(6): 6357–6364
147. Ge C, Lu M, Jian X, Tan Y, Cunningham B T. Large-area organic distributed feedback laser fabricated by nanoreplica molding and horizontal dipping. Optics Express, 2010, 18(12): 12980–12991
148. Liu X, Klinkhammer S, Sudau K, Mechau N, Vannahme C, Kaschke J, Mappes T, Wegener M, Lemmer U. Ink-jet-printed organic semiconductor distributed feedback laser. Applied Physics

Express, 2012, 5(7): 072101
149. Parafiniuk K, Monnereau C, Sznitko L, Mettra B, Zelechowska M, Andraud C, Miniewicz A, Mysliwiec J. Distributed feedback lasing in amorphous polymers with covalently bonded fluorescent dyes: the influence of photoisomerization process. Macromolecules, 2017, 50(16): 6164–6173
150. Karl M, Glackin J M E, Schubert M, Kronenberg N M, Turnbull G A, Samuel I D W, Gather M C. Flexible and ultra-lightweight polymer membrane lasers. Nature Communications, 2018, 9(1): 1525
151. Namdas E, Tong M, Ledochowitsch P, Mednick S R, Yuen J D, Moses D, Heeger A J. Low thresholds in polymer lasers on conductive substrates by distributed feedback nanoimprinting: Progress toward electrically pumped plastic lasers. Advanced Materials, 2009, 21(7): 799–802
152. Pisignano D, Persano L, Visconti P, Cingolani R, Gigli G, Barbarella G, Favaretto L. Oligomer-based organic distributed feedback lasers by room-temperature nanoimprint lithography. Applied Physics Letters, 2003, 83(13): 2545–2547
153. Del Carro P, Camposeo A, Stabile R, Mele E, Persano L, Cingolani R, Pisignano D. Near-infrared imprinted distributed feedback lasers. Applied Physics Letters, 2006, 89(20): 201105
154. Chang J, Gwinner M, Caironi M, Sakanoue T, Sirringhaus H. Conjugated-polymer-based lateral heterostructures defined by high-resolution photolithography. Advanced Functional Materials, 2010, 20(17): 2825–2832
155. Berger V, Gauthier-Lafaye O, Costard E. Photonic band gaps and holography. Journal of Applied Physics, 1997, 82(1): 60–64
156. Yoshioka H, Yang Y, Watanabe H, Oki Y. Fundamental characteristics of degradation-recoverable solid-state DFB polymer laser. Optics Express, 2012, 20(4): 4690–4696
157. Chen S, Zhou Y, Zhai T, Wang Z, Liu D. Different emission properties of a band edge laser pumped by picosecond and nanosecond pulses. Laser Physics Letters, 2012, 9(8): 570–574
158. Stroisch M, Woggon T, Lemmer U, Bastian G, Violakis G, Pissadakis S. Organic semiconductor distributed feedback laser fabricated by direct laser interference ablation. Optics Express, 2007, 15(7): 3968–3973
159. Zhai T, Zhang X, Pang Z, Dou F. Direct writing of polymer lasers using interference ablation. Advanced Materials, 2011, 23(16): 1860–1864
160. Zhang X, Liu H, Li H, Zhai T. Direct nanopatterning into conjugated polymers using interference crosslinking. Macromolecular Chemistry and Physics, 2012, 213(12): 1285–1290
161. Zhai T, Lin Y, Liu H, Feng S, Zhang X. Nanoscale tensile stress approach for the direct writing of plasmonic nanostructures. Optics Express, 2013, 21(21): 24490–24496
162. Scott B, Wirnsberger G, McGehee M, Chmelka B, Stucky G. Dye-doped mesostructured silica as a distributed feedback laser fabricated by soft lithography. Advanced Materials, 2001, 13 (16): 1231–1234
163. Ge C, Lu M, Tan Y, Cunningham B T. Enhancement of pump efficiency of a visible wavelength organic distributed feedback laser by resonant optical pumping. Optics Express, 2011, 19(6): 5086–5092
164. Lawrence J, Turnbull G, Samuel I. Polymer laser fabricated by a simple micromolding process. Applied Physics Letters, 2003, 82 (23): 4023–4025
165. Salerno M, Gigli G, Zavelani-Rossi M, Perissinotto S, Lanzani G. Effects of morphology and optical contrast in organic distributed feedback lasers. Applied Physics Letters, 2007, 90(11): 111110
166. Yamashita K, Takeuchi N, Oe K, Yanagi H. Simultaneous RGB lasing from a single-chip polymer device. Optics Letters, 2010, 35 (14): 2451–2453
167. Kuehne A J C, Gather M C. Organic lasers: recent developments on materials, device geometries, and fabrication techniques. Chemical Reviews, 2016, 116(21): 12823–12864
168. Samuel I D, Turnbull G A. Organic semiconductor lasers. Chemical Reviews, 2007, 107(4): 1272–1295
169. Grivas C, Pollnau M. Organic solid-state integrated amplifiers and lasers. Laser & Photonics Reviews, 2012, 6(4): 419–462
170. Heliotis G, Xia R, Bradley D D C, Turnbull G A, Samuel I D W, Andrew P, Barnes W L. Blue, surface-emitting, distributed feedback polyfluorene lasers. Applied Physics Letters, 2003, 83 (11): 2118–2120
171. Jung H, Han C, Kim H, Cho K S, Roh Y G, Park Y, Jeon H. Tunable colloidal quantum dot distributed feedback lasers integrated on a continuously chirped surface grating. Nanoscale, 2018, 10(48): 22745–22749
172. Zhai T, Wu X, Tong F, Li S, Wang M, Zhang X. Multi-wavelength lasing in a beat structure. Applied Physics Letters, 2016, 109(26): 261906
173. Karnutsch C, Pflumm C, Heliotis G, deMello J C, Bradley D D C, Wang J, Weimann T, Haug V, Gärtner C, Lemmer U. Improved organic semiconductor lasers based on a mixed-order distributed feedback resonator design. Applied Physics Letters, 2007, 90(13): 131104
174. Karnutsch C, Gýrtner C, Haug V, Lemmer U, Farrell T, Nehls B S, Scherf U, Wang J, Weimann T, Heliotis G, Pflumm C, deMello J C, Bradley D D C. Low threshold blue conjugated polymer lasers with first- and second-order distributed feedback. Applied Physics Letters, 2006, 89(20): 201108
175. Zhai T, Tong F, Wang Y, Wu X, Li S, Wang M, Zhang X. Polymer lasers assembled by suspending membranes on a distributed feedback grating. Optics Express, 2016, 24(19): 22028–22033
176. Notomi M, Suzuki H, Tamamura T, Edagawa K. Lasing action due to the two-dimensional quasiperiodicity of photonic quasicrystals with a Penrose lattice. Physical Review Letters, 2004, 92(12): 123906
177. Turnbull G, Andrew P, Barnes W, Samuel I. Operating characteristics of a semiconducting polymer laser pumped by a microchip laser. Applied Physics Letters, 2003, 82(3): 313–315
178. Harwell J R, Whitworth G L, Turnbull G A, Samuel I D W. Green perovskite distributed feedback lasers. Scientific Reports, 2017, 7 (1): 11727
179. Prins F, Kim D K, Cui J, De Leo E, Spiegel L L, McPeak K M, Norris D J. Direct patterning of colloidal quantum-dot thin films for enhanced and spectrally selective out-coupling of emission. Nano Letters, 2017, 17(3): 1319–1325
180. Cao W, Muñoz A, Palffy-Muhoray P, Taheri B. Lasing in a three-dimensional photonic crystal of the liquid crystal blue phase II. Nature Materials, 2002, 1(2): 111–113

181. Yoshino K, Tatsuhara S, Kawagishi Y, Ozaki M, Zakhidov A A, Vardeny Z V. Amplified spontaneous emission and lasing in conducting polymers and fluorescent dyes in opals as photonic crystals. Applied Physics Letters, 1999, 74(18): 2590–2592
182. Shkunov M, Vardeny Z, DeLong M, Polson R, Zakhidov A, Baughman R. Tunable, gap-state lasing in switchable directions for opal photonic crystals. Advanced Functional Materials, 2002, 12 (1): 21–26
183. Kok M H, Lu W, Tam W Y, Wong G K. Lasing from dye-doped icosahedral quasicrystals in dichromate gelatin emulsions. Optics Express, 2009, 17(9): 7275–7284
184. Hirayama H, Hamano T, Aoyagi Y. Novel surface emitting laser diode using photonic band-gap crystal cavity. Applied Physics Letters, 1996, 69(6): 791–793
185. Yang Y, Turnbull G A, Samuel I D W. Hybrid optoelectronics: a polymer laser pumped by a nitride light-emitting diode. Applied Physics Letters, 2008, 92(16): 163306
186. Riedl T, Rabe T, Johannes H H, Kowalsky W, Wang J, Weimann T, Hinze P, Nehls B, Farrell T, Scherf U. Tunable organic thin-film laser pumped by an inorganic violet diode laser. Applied Physics Letters, 2006, 88(24): 241116
187. Heydari E, Buller J, Wischerhoff E, Laschewsky A, Döring S, Stumpe J. Label-free biosensor based on an all‐polymer DFB laser. Advanced Optical Materials, 2014, 2(2): 137–141
188. Haughey A M, Guilhabert B, Kanibolotsky A L, Skabara P J, Dawson M D, Burley G A, Laurand N. An oligofluorene truxene based distributed feedback laser for biosensing applications. Biosensors & Bioelectronics, 2014, 54: 679–686
189. Cao F, Zhang S, Tong J, Chen C, Niu L, Zhai T, Zhang X. Effects of cavity structure on tuning properties of polymer lasers in a liquid environment. Polymers, 2019, 11(2): 329
190. Schneider D, Rabe T, Riedl T, Dobbertin T, Kröger M, Becker E, Johannes H H, Kowalsky W, Weimann T, Wang J, Hinze P, Gerhard A, Stössel P, Vestweber H. An ultraviolet organic thin-film solid-state laser for biomarker applications. Advanced Materials, 2005, 17(1): 31–34
191. Retolaza A, Martinez-Perdiguero J, Merino S, Morales-Vidal M, Boj P G, Quintana J A, Villalvilla J M, Díaz-García M A. Organic distributed feedback laser for label-free biosensing of ErbB2 protein biomarker. Sensors and Actuators B, Chemical, 2016, 223: 261–265
192. Oki Y, Miyamoto S, Maeda M, Vasa N J. Multiwavelength distributed-feedback dye laser array and its application to spectroscopy. Optics Letters, 2002, 27(14): 1220–1222
193. Voss T, Scheel D, Schade W. A microchip-laser-pumped DFB-polymer-dye laser. Applied Physics B, Lasers and Optics, 2001, 73 (2): 105–109
194. Christiansen M B, Schøler M, Kristensen A. Integration of active and passive polymer optics. Optics Express, 2007, 15(7): 3931–3939
195. Vannahme C, Klinkhammer S, Lemmer U, Mappes T. Plastic lab-on-a-chip for fluorescence excitation with integrated organic semiconductor lasers. Optics Express, 2011, 19(9): 8179–8186
196. Toussaere E, Bouadma N, Zyss J. Monolithic integrated four DFB lasers array with a polymer-based combiner for WDM applications. Optical Materials, 1998, 9(1–4): 255–258
197. Ma H, Jen Y, Dalton L R. Polymer-based optical waveguides: materials, processing, and devices. Advanced Materials, 2002, 14 (19): 1339–1365

Yulan Fu obtained her Ph.D. degree from School of Physics, Peking University in 2013. She is currently an associate professor in the College of Applied Science, Beijing University of Technology. Her research interests are mainly focused on on-chip micro-/nano-photonic devices, nonlinear photonic materials and nanostructures.

Tianrui Zhai received his Ph.D. degree from the Department of Physics, Beijing Normal University in 2010. He is currently a professor in the College of Applied Sciences, Beijing University of Technology. His research interests are mainly focused on microcavity lasers, plasmonic physics and devices, and nanophotonics.